JOURNAL OF GEOPHYSICAL RESEARCH, VOL. 93, NO. A1, PAGES 162-174, JANUARY 1, 1988

VLF Wave Stimulation by Pulsed Electron Beams Injected From the Space Shuttle

G. D. REEVES, P. M. BANKS, A.C. FRASER-SMITH, T. NEUBERT, AND R. I. BUSH

Space Telecommunications and Radioscience Laboratory, Stanford University, Stanford, California

D. A. GURNETT

Department of Physics and Astronomy, University of Iowa, Iowa City

W. J. RAITT

Center for Atmospheric and Space Science, Utah State University, Logan

Among the investigations conducted on the space shuttle flight STS 3 of March 1982 was an experiment in which a 1-keV, 100-mA electron gun was pulsed at 3.25 and 4.87 kHz. The resultant waves were measured with a broadband plasma wave receiver. At the time of flight the experimental setup was unique in that the electron beam was square wave modulated and that the shuttle offered relatively long times for in situ measurements of the ionospheric plasma response to the VLF pulsing sequences. In addition to electromagnetic response at the pulsing frequencies the waves exhibited various spectral harmonics as well as the unexpected occurrence of "satellite lines" around those harmonics. Both phenomena occurred with a variety of different characteristics for different pulsing sequences.

1. INTRODUCTION

Many different electron beam experiments have been undertaken with rockets and spacecraft in recent years for a variety of purposes. The pioneering work of Hess [1969], for example, demonstrated that it was possible to create an artificial aurora in the upper atmosphere with a relatively low-power electron beam. Later work by Winckler and his colleagues [*Winckler*, 1980] showed that it was possible to use rocket-borne electron beams to probe successfully the structure of the magnetosphere. Other rocket-borne electron beam experiments have investigated electrical charging phenomena [e.g., *Maehlum et al.* 1980], made measurements of ambient electric fields at geosynchronous orbit [*Melzner et al.*, 1978], and been studied as sources for ELF and VLF radiation arising from modulated beam operation [*Gendrin*, 1974; *Holzworth and Koons*, 1981; *Winckler et al.*, 1984 1985].

The present paper reports the results from low-frequency electron beam pulsing experiments made on the space shuttle flight STS 3. The objective of this work was to increase knowledge of the way a pulsed 1-keV, 100-W electron beam would interact with the ambient ionosphere to produce plasma waves. From a fundamental point of view, the present experiments also investigate the various mechanisms operative in converting the kinetic energy of the electron beam into various types of low-frequency plasma waves, including electromagnetic radiation. In comparison with previous rocket experiments, the shuttle offered a much more extended time period for such operations and, at the same time, permitted observations in a much wider range of ambient plasma conditions. The penalty for using this platform, however, is also important to understand: the shuttle plasma environment is very complex, and the different modes of interaction of the beam with the surface of the shuttle and its surrounding disturbed plasma environment are not well known [*Shawhan et al.*, 1984a, *Banks et al.*, 1987].

The present experiment was flown on the space shuttle on March 22-30, 1982 on the Columbia orbiter as part of the Office of Space Science 1 (OSS 1) mission. Through combined use of the Fast Pulsed Electron Generator (FPEG), which was part of the Vehicle Charging And Potential (VCAP) experiment, and the varied instruments of the Plasma Diagnostics Package (PDP) experiment, approximately 1 hour of data was acquired showing the plasma response to FPEG pulsing at VLF frequencies. These data are the topic of the present paper and are described in detail below. The objectives and results of the later Space Experiment with Particle Accelerators (SEPAC) beam-plasma experiments, which were flown on Spacelab 1, were considerably different and have been described by *Obayashi et al.* [1982], *Akai* [1984], *Sasaki et al.* [1986], and *Neubert et al.* [1986].

The FPEG was fully tested, prior to the OSS 1 mission, in the Johnson Spaceflight Center vacuum chamber. The chamber and experimental setup are described in detail by *Denig* [1982], *Banks et al.* [1982], *Raitt et al.* [1982], and *Shawhan* [1982]. The conditions in the chamber simulated the conditions found at shuttle altitudes with two major exceptions. The neutral gas pressure was 1-2 orders of magnitude higher than the 4.3×10^{-7} torr of the STS 3 ex-

Paper number 7A9097.
0148-0227/88/007A-9097$05.00

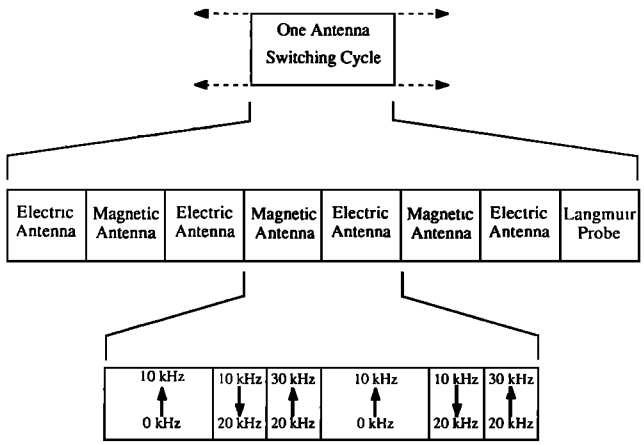

Fig. 1. A schematic representation of the antenna and frequency range switching pattern.

periments. In addition, the chamber was terminated on both ends with a grounded conductor. On the shuttle, of course, the beam was frequently unbounded on one end, and since the shuttle's thermal insulating tiles are also electrically insulating, even when the beam hit a shuttle surface, the boundary conditions were quite different.

One of the primary results of the chamber experiments was the observation of beam plasma discharge (BPD), which was found to occur under almost all chamber conditions, provided the beam current was large enough [*Denig*, 1982; *Banks et al.*, 1982; *Raitt et al.*, 1982]. On STS 3, however, BPD may not have occurred at all and certainly was not a primary effect in the FPEG sequences with short (<0.2 ms) beam emission times [*Banks et al.*, 1987]. This is in agreement with the predictions of *Bernstein et al.* [1982], which suggested that BPD should not occur at the relatively low neutral gas pressures encountered by the orbiter.

2. Experimental Consideration

The Fast Pulsed Electron Generator is a versatile square-pulsed electron beam generator. It was normally operated with a beam energy of 1 keV and a current of 100 mA for a total beam power of 100 W. On a few occasions, however, it was also operated at 50 mA to produce a 50-W beam. The beam half-angle divergence at the FPEG exit is approximately 7.5°. The gun direction is fixed with respect to the orbiter, pointing perpendicularly outward from the payload bay. Both the beam on and off times for the pulses were command controllable. The minimum on or off times were 600 ns, and the maximum on times were 107 s. The beam current had a nominal rise time of 100 ns. Each gun firing, or pulsing period, could contain up to 32,768 pulses. Thus a wide variety of modulation patterns were possible.

The primary diagnostic tool for studying the beam plasma interaction was the University of Iowa Plasma Diagnostics Package (PDP) which contained an array of sensors which are described by *Shawhan* [1984a, Table 1]. The three instruments of principal interest to this investigation were an electric field antenna, a magnetic field search coil and a Low-Energy Proton and Electron Differential Energy Analyzer (LEPEDEA). The ac electric field analyzer and magnetic field search coil were alternately connected to a wideband receiver which was sensitive in the range 10 Hz to 30 kHz. The LEPEDEA is sensative to electrons and positive ions with energies from 2 to 50 eV. During most of the flight the PDP was attached to a pallet in the orbiter cargo bay but during two intervals it was grappled with the Remote Manipulator System (RMS) and moved to selected locations outside the payload bay to distances of 15 m.

Most instruments on the PDP were sampled every 1.6 s. For the electric and magnetic field antennas, however, a continuous recording scheme was used to obtain wideband spectrographic records. The high-resolution spectrum analyzer records two sets of data simultaneously in the ranges 10 Hz to 1 kHz (ELF) and 400 Hz to 10 kHz (VLF). The ELF band recorder switches between the electric and magnetic antennas. The VLF data recording scheme is more complicated. It also follows the electric/magnetic switching pattern, but within each antenna period, three frequency ranges are recorded as follows: 400 Hz to 10 kHz for 25.6 s; then through frequency shifting and inversion, 19.6 to 10 kHz is recorded for 12.8 s; and finally 20.4 to 30 kHz is recorded for 12.8 s. To complicate matters slightly more, every fourth magnetic antenna recording is replaced by a Langmuir probe

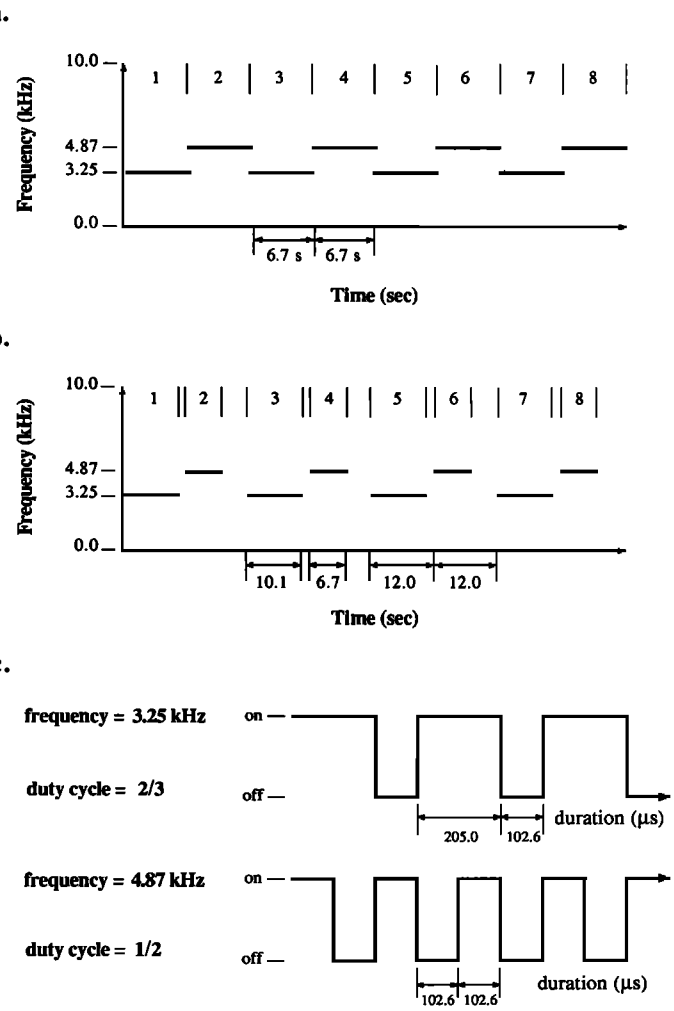

Fig. 2. A schematic representation of the FPEG electron beam VLF pulsing sequence: (*a*) the back-to-back pulsing mode and (*b*) the spaced pulsing mode; (*c*) the waveforms of the two primary pulsing frequencies.

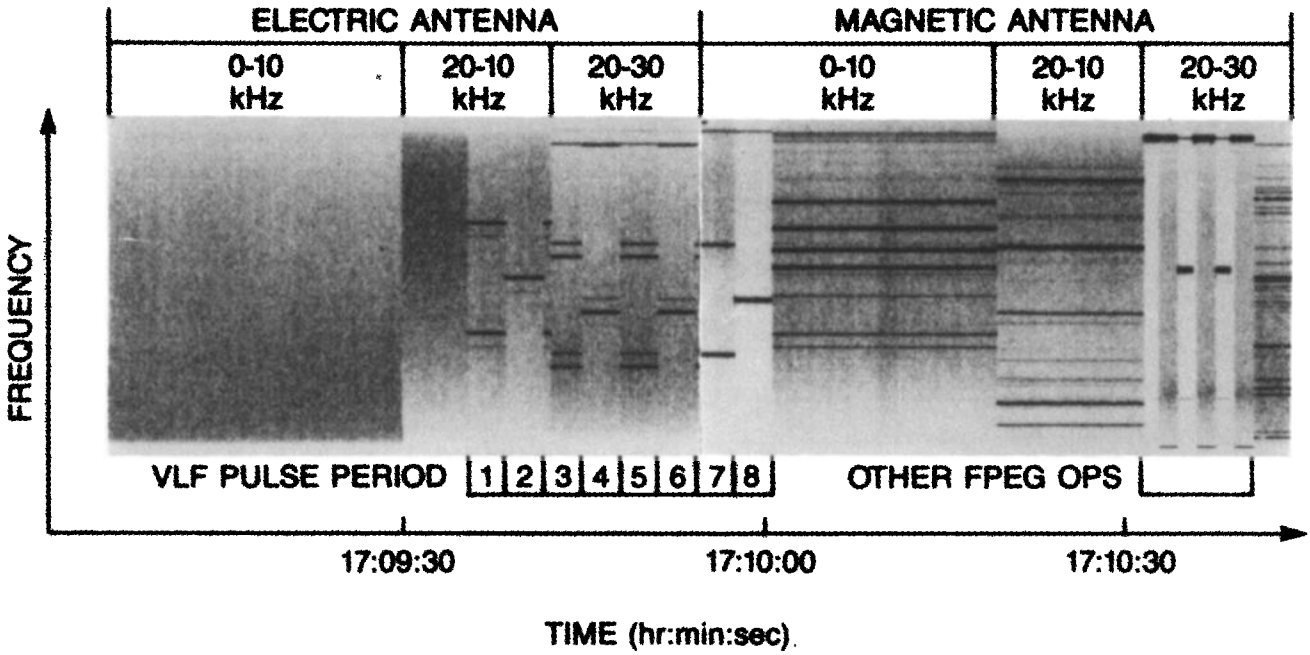

Fig. 3. Wideband data showing wave response to a VLF pulsing sequence superimposed on the antenna switching pattern. Response at the FPEG pulsing frequencies and at harmonics of those frequencies is seen. Other emission features called "satellite lines" are seen associated with some of the harmonic emissions in the 20-10 kHz and 20-30 kHz frequency ranges. FPEG pulsing periods with 3.25 kHz pulsing frequency are even numbered, 4.87 kHz are odd.

recording. (Figure 1 illustrates these sequences.) In the VLF range (0-30 kHz), data were processed into spectrograms made up of sweeps occurring every 25 ms, each consisting of 250 steps of 40 Hz bandwidth and 30 dB of dynamic range.

The antenna switching pattern is persistent in the data and it is important to note that although the data are taken continuously, while one antenna and frequency range is being recorded, the data from the other antenna or the other frequency ranges are lost. Thus there are no continuous electric and magnetic field data for the entire 400 Hz to 30 kHz range.

It is also relevant that the wideband receiver has an Automatic Gain Control (AGC) which operated independently on the ELF and VLF data ranges. The AGC had a 100-dB dynamic range and a response time of about 0.5 s. Values are read out every 1.6 s. It is set according to the integrated wave intensity in the frequency range being recorded at the time. The AGC levels provide information about the total wave intensity as well as allowing comparison of the intensity of emissions in different frequency ranges.

3. Observations

The FPEG was operated in several distinct modulation patterns during the VCAP experiment on STS 3. The modulation patterns are described in detail by *Fraser-Smith et al.* [1985]. The sequences we consider here are the VLF electron beam pulsing sequences. For these, the beam current was set at 100 mA and the gun was pulsed at two primary frequencies: 3.25 and 4.87 kHz. The former had a duty cycle (the ratio of pulse on time to total pulse period) of $\frac{2}{3}$ while the latter had a $\frac{1}{2}$ duty cycle. A typical VLF sequence consisted of eight pulsing periods which alternated between the two frequencies starting with the 3.25 kHz. The details of these sequences are given in Figure 2.

Periods of VLF beam pulsing produced an electromagnetic response which is markedly different from the characteristic background signals during passive conditions. A typical spectrum obtained during passive conditions is dominated by broadband electrostatic noise and discrete spacecraft-generated electromagnetic interference (EMI). During periods of VLF pulsing, relatively strong beam-generated signals are detected at levels of up to 30 dB above the background. [*Shawhan et al.*, 1984b] Both narrowband and broadband signals are generated. The broadband signals are similar to those reported by *Gurnett et al.* [1986]. In this paper we will concentrate on the narrowband signals produced by pulsed electron beam emission. A short time ($\approx$ 0.5 s) after the beam pulsing begins, the AGC reduces the overall gain, thus suppressing the background noise. As Figure 3 illustrates, what is then observed in intensity spectrograms is reduced background noise with eight pulsing periods in which the fundamental firing frequencies and some of their harmonics appear as distinct spectral lines. Which lines are detectable depends, in part, on which parts of the antenna switching pattern the VLF sequence spans.

During the STS 3 mission, broadband spectral data were obtained for 48 VLF sequences producing approximately 1 hour of VLF wave stimulation data. For each of these 48 sequences, discrete emissions were detected at both fundamental pulsing frequencies and at harmonics of those frequencies. This is in agreement with the theory that an electron beam square wave pulsed at VLF frequencies will produce discrete emissions at the pulsing frequency and its harmonics which can propagate in the whistler and the slow and fast Alfvén modes [*Harker and Banks*, 1983, 1985] How-

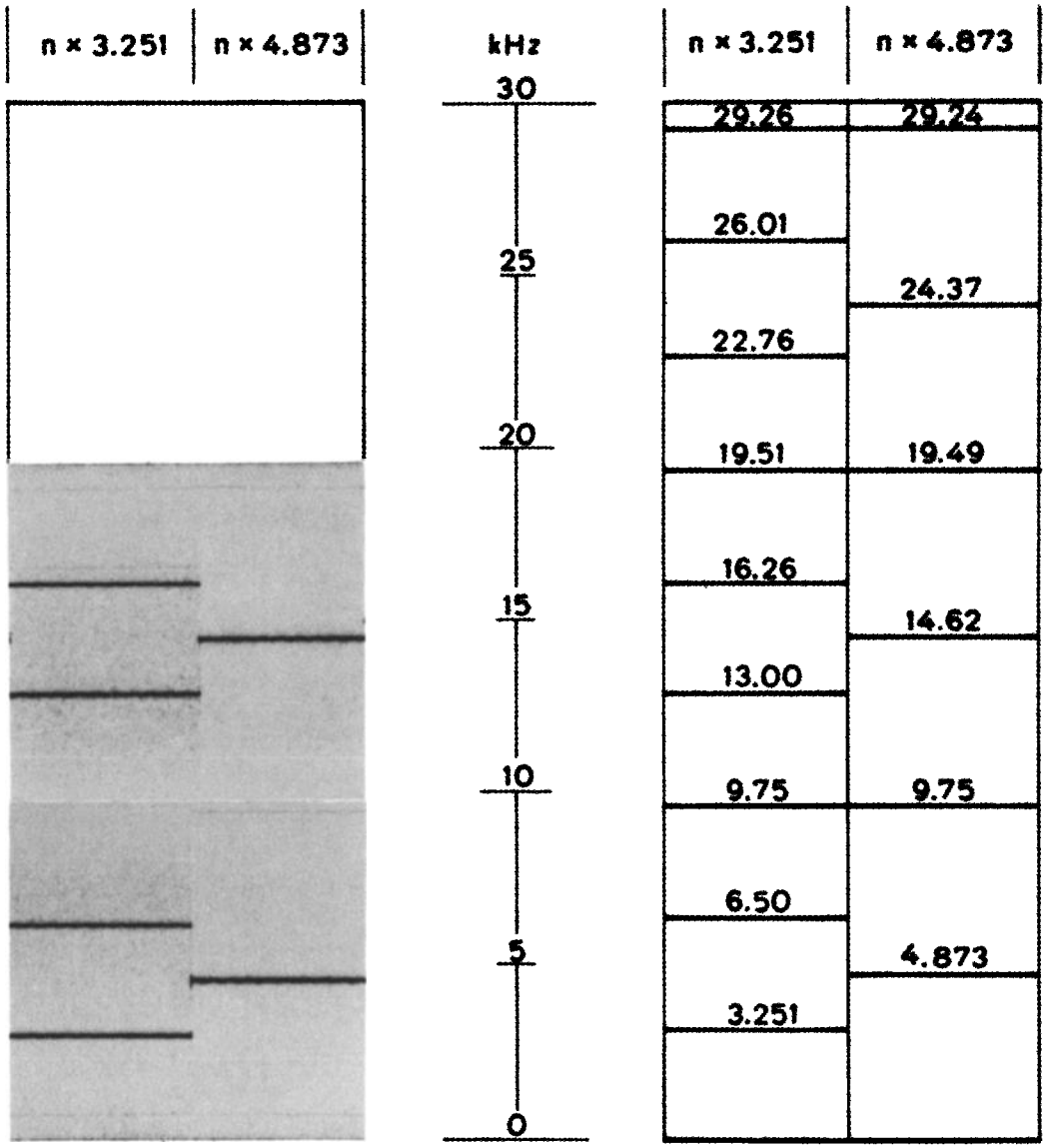

Fig. 4. A spectrogram which agrees well with theory. Narrow-band emissions are seen at the gun pulsing frequencies and at harmonics of those frequencies. Lines with integral $n(b/d)$, called "forbidden frequencies," are not observed.

ever, it cannot be determined if the emissions produced by the VLF sequences are propagating waves using the wide-band wave receiver on the PDP because the PDP was at all times within 15 m of the FPEG and therefore well within the near-field region. No qualitative difference was seen between the VLF pulsing sequences for which the PDP was in the payload bay and sequences for which it was attached to the manipulator arm. In addition, attempts to detect whistler mode emissions during magnetic conjunctions from the Dynamics Explorer 1 (DE 1) satellite, at distances of up to several thousand kilometers, did not produce conclusive results. (Magnetic conjunction during FPEG operations was achieved for 12 cases, but in all but two of those, the DE satellite was outside the region of whistler mode propagation as determined through ray-tracing techniques. For the two other cases the electron beam was known to have hit the STS 3 orbiter within one gyroperiod [*Inan et al.*, 1984].)

During the VLF sequences many other phenomena can be seen in addition to the discrete emissions at the pulsing frequencies. A variety of interesting results can be broadly classified under the two categories "harmonic structure" and "satellite lines." A third category, which may be related to the second, can be called "subharmonics." These will be examined in detail below and analyzed in the following section.

Harmonic Structure

The VLF wave stimulation experiment produced wave response at the gun pulsing frequencies of 3.25 and 4.87 kHz and at integral multiples of those frequencies. The amplitudes of these harmonic spectral lines varied from one sequence to another, but they were present in every pulsing sequence at frequencies up to the 30-kHz limit of the PDP wave receiver. The 3.25-kHz firings have nine harmonics which fall in the 0-30 kHz range and the 4.87-kHz firings

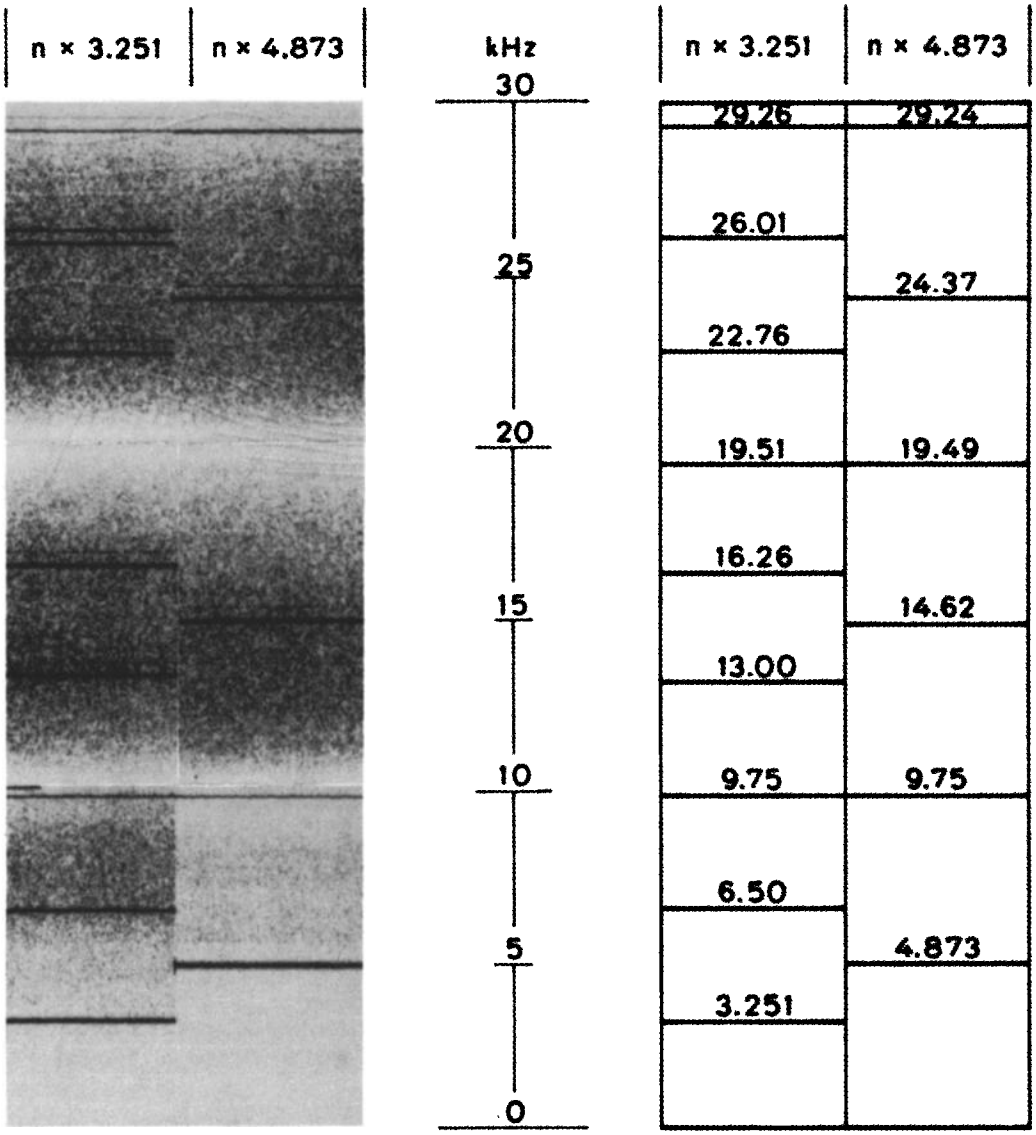

Fig. 5. A spectrogram showing the presence of lines at "forbidden frequencies" as well as "satellite lines" associated with the harmonic spectral lines at the higher frequencies.

have six. These frequencies have particularly simple duty cycles (ratio of beam on time to total period) of $\frac{2}{3}$ and $\frac{1}{2}$, respectively. The choice of these frequencies gives common harmonics at nearly 9.75, 19.75, and 27.24 kHz. For a pulsed electron beam with the given choices of duty cycle, power spectrum theory also predicts that these frequencies (the so-called "forbidden frequencies") should not appear for either pulsing frequency.

Figure 4 illustrates a spectrum with a normal harmonic structure. It was constructed by taking the broadband data (as in Figure 3) and ordering it to remove the complexity of the antenna switching pattern. Although the 20-30 kHz data were not available for this sequence, we see that there are strong emissions at the fundamental pulsing frequencies and their harmonics and no appreciable signals at the "forbidden frequencies."

In contrast to the predictions of theory, our experimental results indicate that in a surprising number of cases, the harmonic spectral lines include the "forbidden frequencies." Figure 5 shows such a situation. In fact, in approximately 60% of the VLF sequences, the 9.75-kHz line was present with an amplitude which ranged from as low as 30 dB below the amplitude of the fundamental to cases in which it was actually more intense. Cases of spectra which generally include the "forbidden frequencies" and cases which do not are seen with both the electric and magnetic antennas, and there seems to be little difference in the morphology of the response of the two fields.

Unfortunately, instrumental limitations complicated the complete analysis of the presence of the "forbidden frequencies." Sensitivity roll-off at the lower end of the recorded frequency range makes it impossible to measure signals near 19.75 kHz which corresponds to the sixth harmonic of the $\frac{2}{3}$ duty cycle pulsings and the fourth harmonic of the $\frac{1}{2}$ duty cycle pulsings. (Recall that the 10-20 kHz band is inverted for recording.) The signals near 9.75 and 27.24 kHz have no such difficulty since the instrument was sensitive to within a few hertz of 10 kHz. The lines at 27.24 kHz, which are the

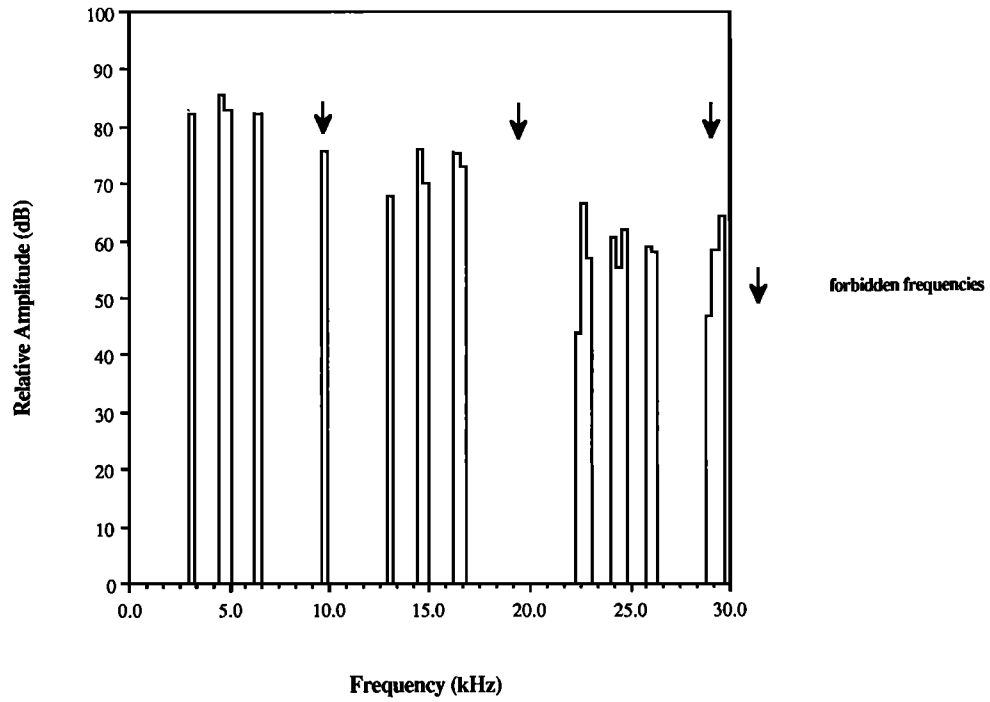

Fig. 6a. Relative amplitude of the spectral lines as measured by the electric antenna.

ninth harmonic of the $\frac{2}{3}$ pulsings and the sixth harmonic of the $\frac{1}{2}$ pulsings, are, however, obscured by an interfering signal probably produced by the FPEG power converter. This EMI is detectable with both the electric and magnetic antennas when the PDP is stowed on the OSS 1 pallet and is detectable primarily with the magnetic antenna when the PDP is deployed on the manipulator arm. The principal effect of this line is to make it difficult to determine if the harmonics at 27.24 are present or not. Thus we are limited in our studies of "forbidden frequencies" to the signals at 9.75 kHz.

Figure 6 shows the relative amplitude of the spectral components observed with the electric and magnetic antennas. The plots were constructed by splitting the 30-kHz band

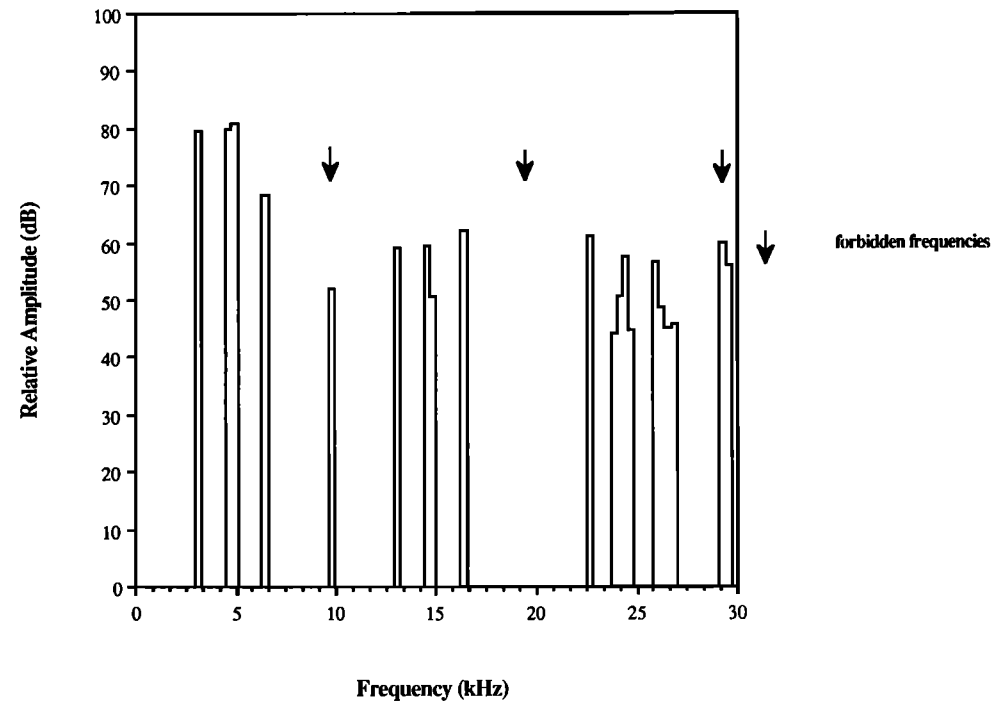

Fig. 6b. Relative amplitude of the spectral lines as measured by the magnetic antenna.

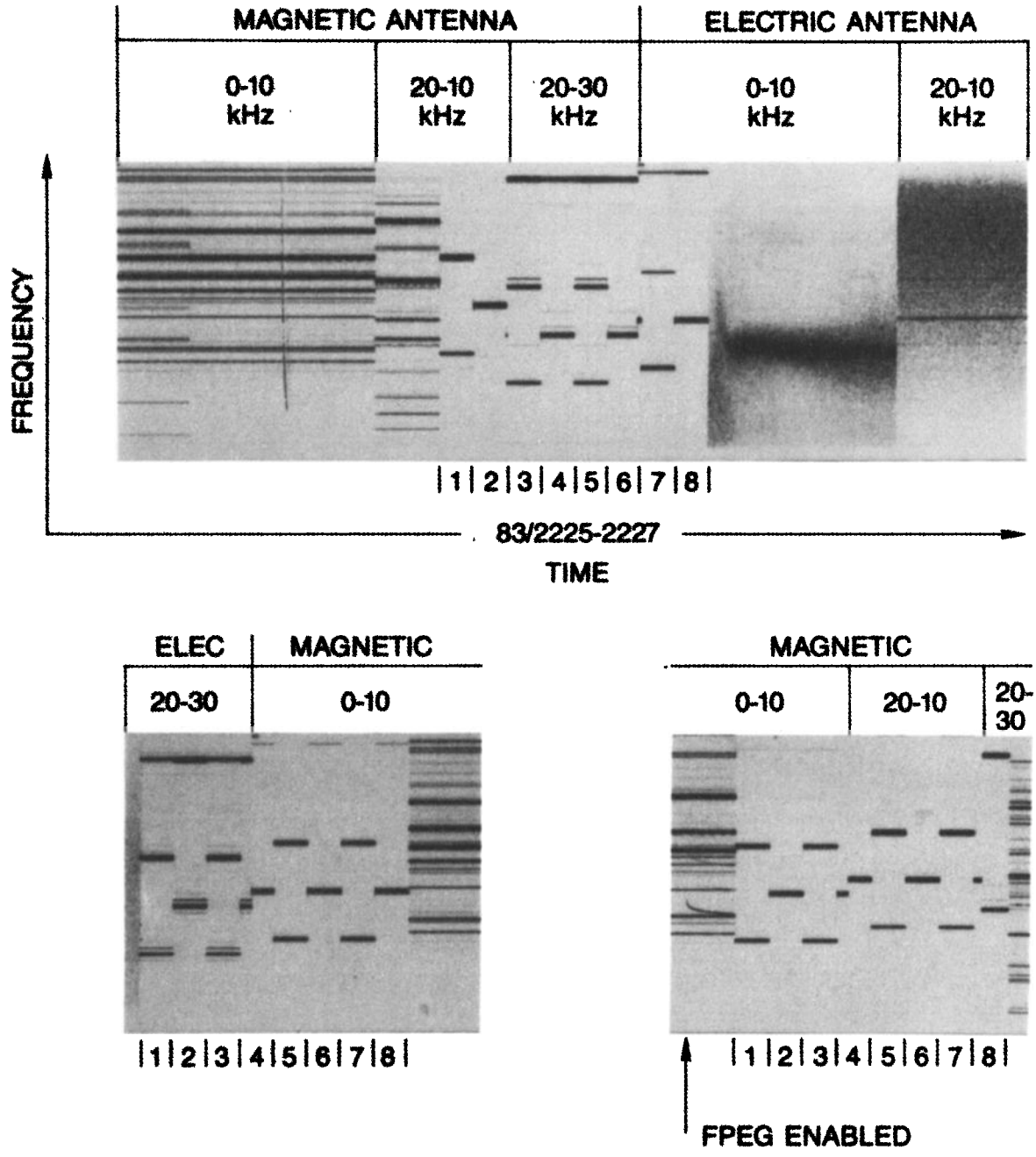

Fig. 7a. Spectrograms, with antenna switching pattern included, showing a variety of manifestations of satellite lines and including single satellite lines of higher frequency as seen in the first spectrogram in pulsing periods 3-6, satellite lines of both higher and lower frequency as in the second spectrogram in the lower harmonics of pulsing periods 1-4, and broadened line emissions as seen in the second and third spectrograms at various harmonics.

into one hundred 300-Hz bands and averaging the contributions from seven typical sequences. Many of these sequences had satellite lines (described later), which accounts for the apparent broadening of the lines. We also note that the broadband receiver provides only relative amplitudes between similar antennas: the electric and magnetic relative amplitudes cannot be compared with each other, although one electric or magnetic spectrum can be compared with another like spectrum. Further, the amplitudes at 27.24 kHz must be considered an estimate because of the presence of EMI. Within these limits of interpretation we see that the averaged amplitude of the spectral components generally decreases slowly with increasing frequency and that there is significant decrease in amplitude at the "forbidden frequencies." The fact that there is a response at those frequencies indicates the presence of VLF sequences which have lines at the "forbidden frequencies."

Satellite Lines

Another interesting and unexpected phenomenon observed in the STS 3 broadband VLF data obtained during

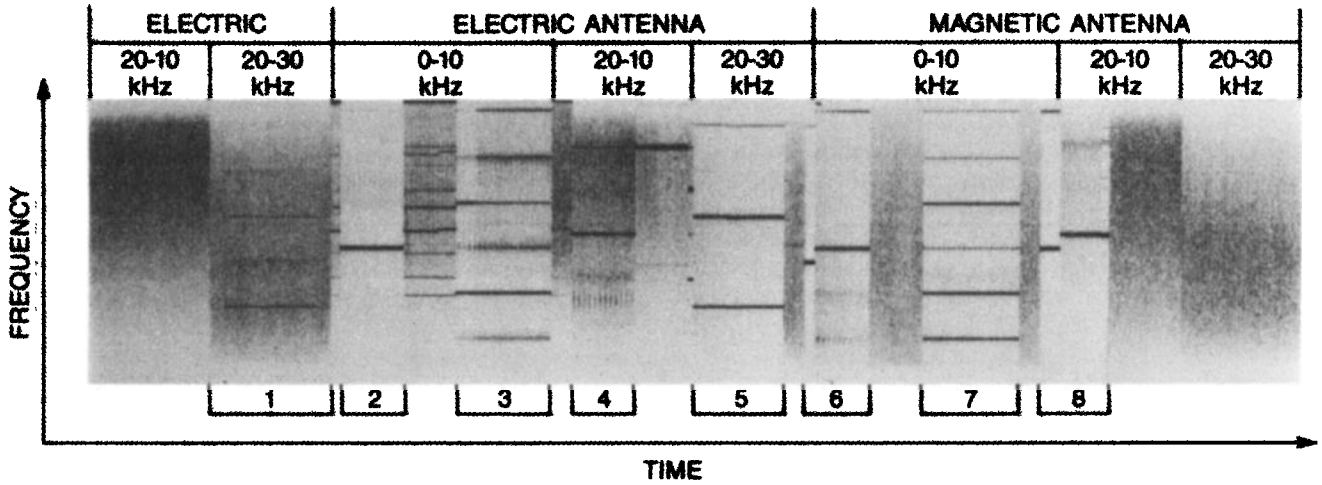

Fig. 7b. A spectrogram, with antenna switching pattern included, showing emissions at half integral multiples of the pulsing frequency which occur during pulsing periods 3 and 7.

FPEG pulsing sequences was the presence of "satellite lines" situated near the various harmonic spectral lines. To our knowledge, this is a previously unobserved effect. It is characterized by one or more emissions separated in frequency from the harmonic spectral lines produced by the pulsed electron beam. The separation can range from 100 Hz to over 1 kHz. satellite lines were detected in 26 out of 48 sequences. In seven of those 48 cases, measurements in the 20–30 kHz frequency range were not obtained. Since satellite lines are most frequently observed in the 20–30 kHz range, no conclusions can be drawn for these seven cases.

The most common type of satellite line is a single subsidiary line which is higher in frequency than its primary. Figure 5 shows a typical spectrum with a single satellite line of higher frequency associated with some of the harmonic spectral lines. Of the 26 sequences with satellite lines, 10 were of this type. They occur mainly in the 20–30 kHz range but are also seen between 10 and 20 kHz and, rarely, in the 0–10 kHz range. In general, all satellite lines in a given observational period have the same frequency separation from their associated harmonic lines for each harmonic. There are, however, notable exceptions. The strength of the satellite lines is also highly variable. It is intriguing to note that the satellite lines occur as soon as the firing is detected, which is instantaneous within measurement limitations: no buildup is detected. The satellite lines also disappear, with the primary lines, when the gun is turned off.

Figure 7 shows some of the other varieties of satellite lines. Of these, the most common are satellite lines of both higher and lower frequency. Sometimes several pairs of satellite lines will surround a given harmonic. Another variation is the presence of a narrow noise band around the primary spectral lines. Intensity maxima and minima may indicate the development of satellite lines but the lack of sufficient cases makes this uncertain. It is also possible to have narrow bands and distinct lines around the same primary line.

An even more unusual case of the presence of spurious emissions is seen in Figure 7b during the pulsing periods labeled 3 and 7. At those times, Figure 7b shows one of two sequences in which "half integral harmonics" were seen. It is not thought that these are satellite lines with large frequency separation in part because these lines change in intensity during a firing.

In passing we note that a variable frequency emission associated with enabling high voltage to the FPEG is also seen prior to electron emission. This emission is seen, for example, in Figure 7 at the point marked "FPEG enabled" and between 800 and 900 Hz in Figure 9 prior to the appearance of subharmonics. It is fairly common and is associated with enabling of the FPEG filament high voltage before a pulsing sequence begins. It generally appears in the magnetic antenna. Since these emissions are clearly instrumental in origin and do not appear to be related to any of the other observed features, they have not been the subject of extensive investigation.

Figure 8 shows the distribution of the frequency separation (Δf) between a satellite line and its primary. Several features are evident. First, cases which have satellite lines at higher frequencies ($\Delta f > 0$) are more common (particularly at 400 Hz). The most common separations have 70 Hz $\leq |\Delta f| \leq$ 160 Hz. Separations this small do not appear as distinct lines on the spectrographic films but, rather, as broadened dark lines. Amplitude scans of the data obtained from analysis of the original magnetic tapes do reveal signals at these frequency separations. We note also that for those separations, there is almost always a pair of lines with one higher and one lower in frequency than the primary.

Subharmonics

A third type of emission feature has been identified in the 0-1 kHz (ELF) broadband data which was recorded simultaneously with the 0-30 kHz (VLF) data. For want of a better name, we have termed these "subharmonics". They are illustrated in Figure 9 along with the same sequences seen in the 0-30 kHz range. The subharmonics, like the harmonic spectral lines, are narrowband, begin and end with the pulsing period, and have reasonably constant amplitude during a pulsing period. Several features are striking. First, we note that the frequency of the subharmonics decreases with time. The rate of decrease is of the order of 1-2 Hz/s. (No correlation was found with the fractional change per unit time of the subharmonic frequency and the STS 3 orbital environ-

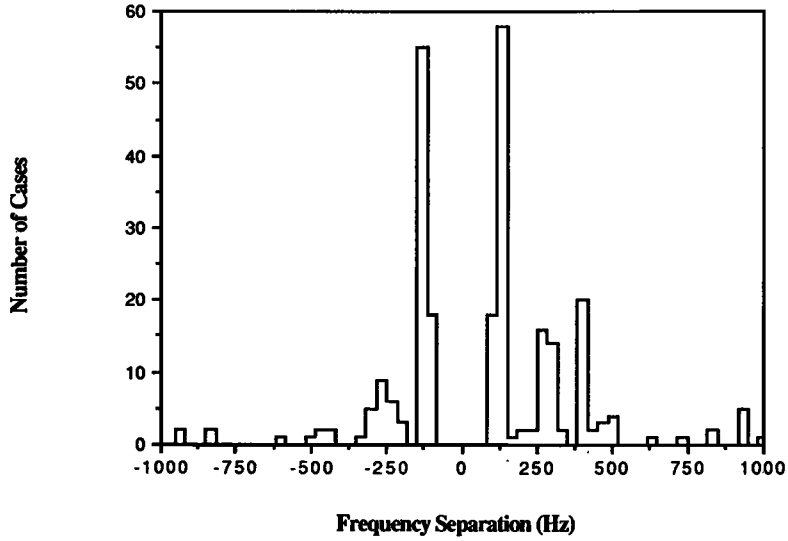

Fig. 8. The distribution of frequency separation, Δf , between a primary spectral line and its satellite line is shown. The number of cases refers to the total number of lines with such a separation, not the number of pulsing periods.

ment parameters, however.) At least six sequences, including two of those of Figure 9, clearly display pairs of subharmonics. Regardless of the frequency of the subharmonic or the frequency of the fundamental, the higher-frequency subharmonic spectral line is twice the frequency of the lower. This leads us to conclude that the higher frequency lines are the second harmonic of the lower. A third harmonic or higher was never observed. Since spectral lines at the pulsing frequencies are not observed to drift in frequency, the ratio of pulsing frequency to subharmonic frequency is nonintegral and time varying. Further, the ratio of the pulsing frequency to the subharmonic ELF frequency is different for the 3.25- and 4.87-kHz firings.

4. DISCUSSION

Harmonic Structure

Harker and Banks [1983, 1985] presented a simple model for the far-field radiation expected from a pulsed electron beam in a magnetized plasma. This theory predicts that the beam will radiate at the pulsing frequency and at harmonics of that frequency in the whistler and the slow and fast Alfvén modes. *Harker and Banks, [1986]* later expanded that work to include contributions from the near field as well. In both cases, the power in the fields for each harmonic n was found to be proportional to the term $sin^2(n\pi(b/d))$ where b/d is

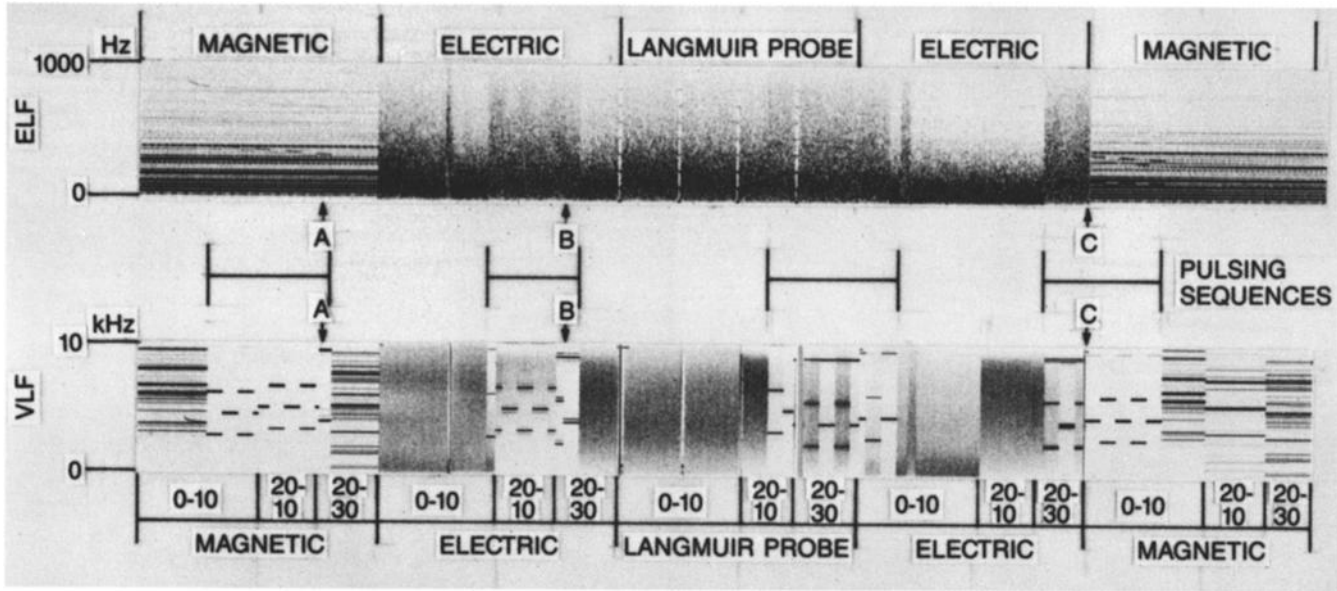

Fig. 9. Spectrograms, with antenna switching pattern included, are shown in (*a*) the ELF (0-10 kHz) and (*b*) the VLF (0-30 kHz) ranges. Good correlation between the frequency of the subharmonics in Figure 9a and the frequency separation of the satellite lines in Figure 9b is illustrated. At the points marked A, B, and C the subharmonic frequencies are 330, 250, and 163 Hz, respectively. The frequency separation of the satellite lines from the harmonics of the pulsing frequencies at those points are 330, 267, and 150 Hz.

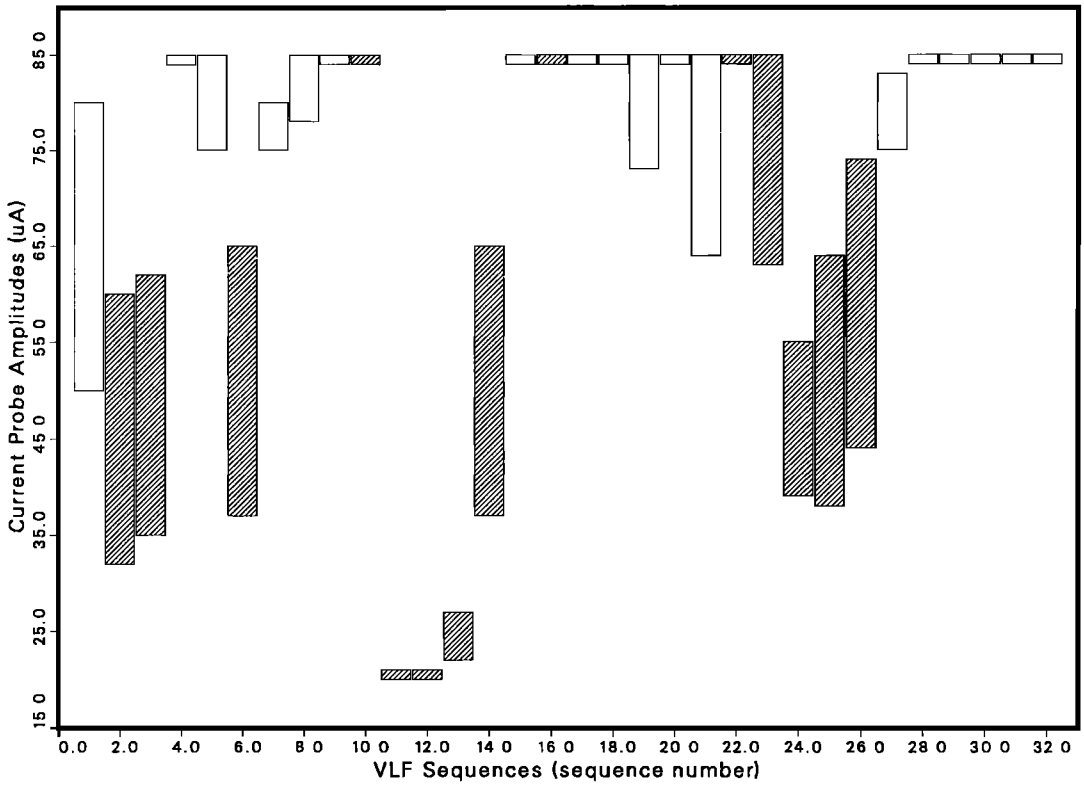

Fig. 10a. The range of return current collected by the CP1 instrument is shown for each sequence which had wideband data in the 20-30 kHz frequency range of the electric antenna. Sequence number is as they occurred in time during the mission and should be considered schematic.

the duty cycle of the pulse. The expected amplitude of the harmonics is considerably more complicated and the reader is referred to their papers, but one feature is quite striking. For integral $n(b/d)$, the amplitudes go to zero. Thus, as in Figure 3, for the $\frac{2}{3}$ duty cycle firings (3.25 kHz) the third, sixth, and ninth harmonics should be missing, and for the $\frac{1}{2}$ duty cycle (4.87 kHz) all the even harmonics should vanish.

For both fundamental pulsing frequencies, the vanishing harmonics correspond to 9.75, 19.75 and 27.24 kHz, hence the term "forbidden frequencies." These frequencies are, of course, forbidden only for our particular choice of pulsing parameters and are a result, in part, of the Fourier decomposition of the given waveform. As Figures 4-6 indicate, our data conformed with theory in many cases but deviated from that theory for the majority of VLF sequences.

Efforts have been made to isolate the physical factors which give rise to the presence of unexpected harmonics. However, no correlation was found between the amplitude of the harmonics and the best estimated trajectory (BET) environmental parameters, which include the magnetic field vector, the ram (or antivelocity) vector, altitude, latitude, longitude, L shell, and a day/night parameter. In addition, there were the calculated variables such as electron beam column radius (electron gyroradius), the electron beam column center to detector distance, the $\mathbf{V}\times\mathbf{B}$ vector, and a shuttle hit/miss parameter. Two-variable scatter plots were made for each pair of parameters and sequences with particular spectral characteristics given different symbols to determine if there was a preferred region of, or trajectory in, parameter space which contained the sequences which conformed to theory and another region, or trajectory, which contained those which did not. Due, in part, to the fact that many parameters covered only a small part of their total possible range, the results were ambiguous, and no correlations could be found for any of the above mentioned parameters. We can conclude, then, that the factor controlling the presence of lines at the "forbidden frequencies" is variable but is not a simple function of the orbiter environment.

We have also investigated the possibility that the variation in harmonic structure arises from an instrumental effect. However, the lack of any correlation between primary signal intensity and presence of the forbidden harmonics argues strongly against this possibility. A more likely possibility is a degradation of the electron beam radiation condition such that the assumption of beam coherence used by *Harker and Banks*, [1983, 1985, 1986] is violated. If, for example, each pulse radiated only at the leading or trailing ends, the spectrum obtained would contain uniform harmonics of equal amplitude. Work is now proceeding to extract the phase information from the spectrogram in an attempt to reconstruct the effective radiating portion of the pulse and to determine what parameters would change the effective pulse shape.

Satellite Lines and Subharmonics

We have grouped satellite lines and subharmonics under the same section at this point because we have reason to believe that the presence of subharmonics and the presence of satellite lines are related to the same physical phenomenon,

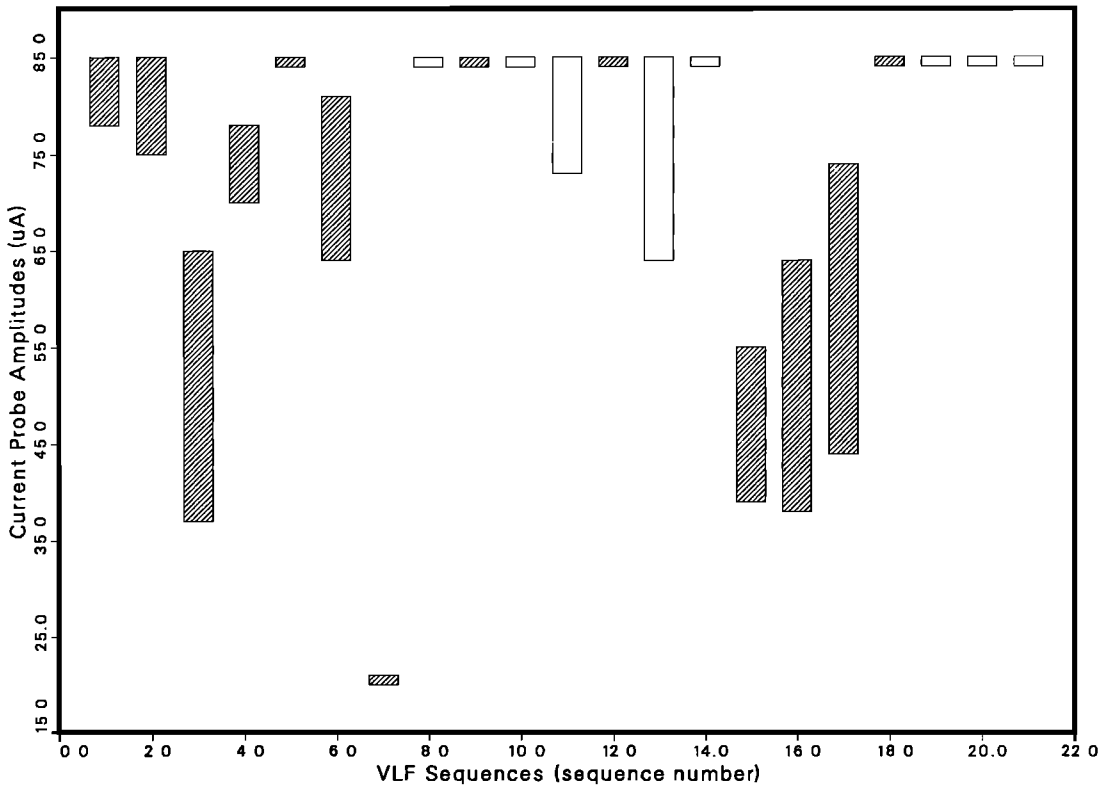

Fig. 10b. The same as Figure 10a but for sequences which had wideband data in the 20-30 kHz frequency range of the magnetic antenna.

and it becomes redundant to discuss them separately. Out of 43 VLF sequences with complete (ELF and VLF) data, 19 sequences had neither satellite lines nor subharmonics while 18 had both satellite lines and subharmonics and only six had either satellite lines or subharmonics but not both. Of the 18 sequences with satellite lines and subharmonics, 13 had subharmonics with frequencies comparable to one or more frequency separations for the satellite lines ($\Delta f \approx f_{sub}$). It should be noted that of that 13, nine had additional satellite lines or subharmonics with no counterpart. To complete the inventory, five sequences had satellite lines and subharmonics but $\Delta f \neq f_{sub}$. Further evidence of the relationship between satellite lines and subharmonics is seen in Figure 9. Comparing three points in the series of firings (labeled A,B, and C in Figure 9) we find subharmonic frequencies of 330, 250, and 163 Hz, respectively. (All with an error of ±10 Hz.) For the satellite lines, we find that the difference frequencies (Δf) at the same points are 330, 267, and 150 Hz (all ±33 Hz). The agreement is quite good but can not be compared for all sequences because of complications arising from the VLF antenna switching pattern. The ELF wave data are continuously displayed for 0-1 kHz, but the VLF antenna switching provides data in the 20-30 kHz range, where satellite lines are most commonly observed, only for one quarter of the time. Thus the full temporal development of the satellite lines cannot be observed.

Examination of data from the VCAP current probes and the LEPEDEA indicates that the orbiter electrical return current is involved in the interaction. Figure 10 shows the data from the current probe 1 (CP1). The ordinate is the peak current measured in each sampling period of 17 ms. The area of the detector is 0.05 m^2 and the current is measured in microamperes. The saturation value for the detector was 85 μA. The CP1 values shown here indicate the peak flux of electrons minus ions collected on the detector surface. The bars in Figure 10 indicate the range of peak currents detected during one pulsing sequence with shaded bars indicating sequences with satellite lines. We see that for times when the pulsing sequence overlaps the times when the 20-30 kHz range is monitored, satellite lines tend to occur for relatively low values of the return flux of electrons measured by CP1, which is located next to the FPEG. There is no correlation with the current collected by CP2, which is located several meters away from the FPEG on the opposite side of the OSS 1 pallet. (See Figure 11.) The current collected at this probe appears to be controlled by ambient plasma flow which is, in turn, controlled by the attitude of the orbiter, the orbiter plasma environment, and the orbiter-plasma potential. Figure 11 shows the relative positions of the FPEG, PDP, and the CCP 1 and CCP 2 instruments. The projection of the beam column onto the plane of the payload bay is also shown shaded for a typical magnetic field configuration.

In contrast to the current probes, the LEPEDEA tended to measure larger fluxes of hot electrons at times when satellite lines were observed. The PDP was located 1.55 m away from the FPEG on the forward part of the OSS 1 pallet, and electrons did not reach it by following unperturbed helical trajectories. If the electrons spread along the magnetic field direction, the helix becomes a cylindrical shell with its axis along the magnetic field. We were surprised to find that our analysis indicates that the PDP was outside this beam column for all the VLF sequences for which the PDP was mounted in the payload bay. (When the PDP was on the manipulator arm, its position was not known.)

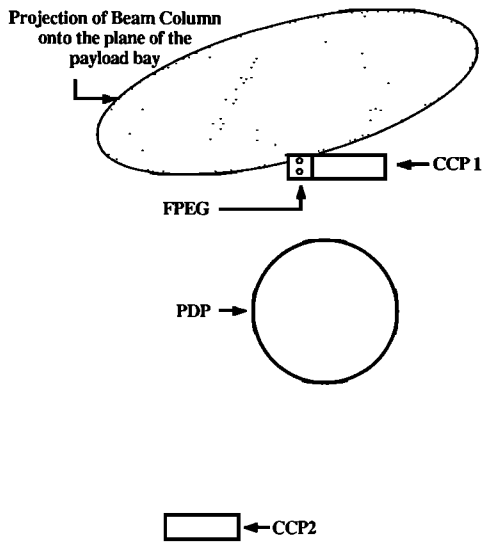

Fig. 11. The relative positions of the Fast Pulsed Electron Generator, the Plasma Diagnostics Package, and the charge and current probes. Also shown as a shaded ellipse is the column formed by the gyromotion of the electron beam projected onto the plane of the payload bay for a typical magnetic field strength and direction.

There does not appear to be any correlation between distance to the beam column and the presence or strength of satellite lines. We conclude then that the LEPEDEA does not measure freely escaping beam electrons but rather energetic electrons coming from collisions, coulombic expansion of the beam, or some undetermined instability which drives electrons perpendicular to the magnetic field. This occurs at the same time that the number of electrons traveling toward the FPEG, as measured by CCP 1, is reduced. Hence we are led to suspect a process which reduces the number of electrons scattered back along the field lines and scatters them, instead, perpendicular to the field lines. These results indicate a strong beam plasma interaction.

We have taken care to avoid calling the satellite lines "sidebands," which would imply conventional mechanisms such as amplitude or frequency modulation, linear beating with an undetected frequency, or some aliasing mechanism. We have considered these mechanisms but have found that none can explain the complexities in the data. The electron beam was modulated in a simple pulsed mode producing a square wave modulated current source. If there is any coherent amplitude or frequency modulation of the source, it would necessarily imply a beam plasma interaction. Both the linear beating and the aliasing possibilities are unlikely because the VLF and ELF wave receiver channels are independent and have separate cutoff filters. We believe that the correlation between the frequency separation of the satellite lines and the frequency of the subharmonics rules out those processes. Further, aliasing would not account for the gradual drift in frequency of the satellite lines and subharmonics. We rule out Doppler shift for the simple reason that the source and the receiver are comoving. If any additional argument was needed, one could note that Doppler shifting would not produce subharmonics through any linear mechanism. The possibility of problems caused by the heterodyning of the signal was also considered because the satellite lines occur most often in the 10-20 and 20-30 kHz bands which are heterodyned by the broadband receiver down to the 0-10 kHz range. The fact that the subharmonics appear for the duration of a pulsing sequence argues against this possibility. The ELF channels are not heterodyned and are subject to only the electric/magnetic switching pattern. Further, aliasing would not account for the gradual drift in frequency of the satellite lines and subharmonics. We have been unable to determine any other instrumental effect which could satisfactorily explain the presence of these emission features.

A possible explanation may be that under certain conditions, the electron beam creates a hot plasma environment in the payload bay and any one of the many orbiter instruments could induce a periodic disturbance in that plasma which could then interact, in an undetermined manner, with the beam-generated signals. This possibility is given added weight when one notices the presence of satellite lines with $\Delta f = 400 \pm 33$ Hz in three VLF sequences around a total of 20 individual primary lines and that the AC power available on the orbiter was at 400 Hz. It should be noted that although a subharmonic at approximately 400 Hz was detected for each of those three VLF sequences, no subharmonic near 400 Hz was detected in any of the 40 other sequences.

5. CONCLUSIONS

In summary, our primary observation was the existence of a narrowband electromagnetic response detected at the pulsing frequencies of 3.25 and 4.87 kHz. In addition, narrowband lines were seen at harmonics of those frequencies. The harmonic structure often deviated from predictions, but the causes for those deviations are, as yet, unknown. Another prominent feature which was frequently observed in the spectra was the presence of "satellite lines" which appear to be related to the presence of energetic electrons around the PDP as measured by the LEPEDEA and a corresponding decrease in current flow to the orbiter near the FPEG. "subharmonics" were observed during VLF sequences at frequencies far below the fundamental pulsing frequencies. There is statistical evidence that they are part of the same phenomenon which produces the "satellite lines." The exact nature of that phenomenon and the cause of the deviation of the primary harmonic structure from theory are areas of ongoing research.

Acknowledgments. The authors would like to acknowledge the contribution of D. Gurnett and L. Frank of the University of Iowa in providing data from the Plasma Diagnostics Package instruments and the valuable assistance of K. Harker and J. Yarbrough of Stanford University. This work was supported under grants NAGW-235 and RADC F19628-84-K-0014 at Stanford University.

The Editor thanks K.N. Erickson and D.N. Walker for their assistance in evaluating this paper.

REFERENCES

Akai, K., Electron beam-plasma interaction experiment in space, ISAS Res. Note 285, Inst. of Space and Astronaut. Sci., Tokyo, 1984

Banks, P.M., W.J. Raitt, and W.F. Denig, Studies of beam-plasma interactions in a space simulation chamber using prototype space shuttle instruments, in *Artificial Particle Beams in Space Plasma Studies*, edited by B. Grandal p.393, Plenum, New York, 1982.

Banks, P.M., W.J. Raitt, A.B. White, R.I. Bush, and P.R. Williamson, Preliminary results from the Vehicle Charging and Potential experiment on STS 3, *J. Spacecr. Rockets*, in press 1987.

Bernstein W., P.J. Kellog, S.J. Monson, R.H. Holzworth, and B.A. Whalen, Recent observations of beam-plasma interactions in the ionosphere and a comparison with laboratory studies of the beam plasma discharge., in *Artificial Particle Beams in Space Plasma Studies*, edited by B. Grandal, p.35, Plenum, New York, 1982. Plenum Press, NY, 1982.

Denig, W.F., Wave and particle observations associated with the beam plasma discharge in a space simulation chamber., PhD. thesis, Utah State Univ., Logan, 1982.

Fraser-Smith, A.C., P.M. Banks, and G.D. Reeves, Observations of sub-LF electromagnetic field phenomena associated with modulated electron beams on STS 3, *Final Tech. Rep. RADC-TR-85-152*, Rome Air Force Dev. Cent., Griffiss AFB, New York, Aug. 1985.

Gendrin, R., The French-Soviet ARAKS experiment, *Space Sci. Rev., 15*, 905, 1974.

Gurnett, D.A., W.S. Kurth, J.T. Steinberg, P.M. Banks, R.I. Bush, and W.J. Raitt, Whistler-mode radiation from the spacelab-2 electron beam, *Geophys. Res. Lett., 13*, 225, 1986.

Harker, K.J., and P.M. Banks, Radiation from pulsed electron beams in space plasmas, *Radio Sci., 19*,(2), 454, 1983.

Harker, K.J., and P.M. Banks, Radiation from long pulse train electron beams in space plasmas, *Planet. Space Sci., 33*, 953, 1985.

Harker, K.J., and P.M. Banks, Near fields in the vicinity of pulsed electron beams in space, *Planet. Space Sci., 35*, 11, 1986.

Hess, W.N., Generation of artificial aurora, *Science, 164*, 1512, 1969.

Holzworth, R.H., and H.C. Koons, VLF Emissions from a modulated electron beam in the auroral ionosphere., *J. Geophys. Res., 86*, 853, 1981.

Inan, U.S., M. Pon, P.M. Banks, P.R. Wiliamson, W.J. Raitt, and S.D. Shawhan, Modulated beam injection from the space shuttle during magnetic conjunctions of STS 3 with the DE 1 satellite, *Radio Science, 19*(2), 487, 1984.

Maehlum, B.N., K. Maseide, K. Aarsnes, A. Egeland, B. Grandal, J. Holtet, T.A. Jacobsen, N.C. Maynards, F. Soraas, J. Stadsnes, E.V. Thrane, and J. Troim, Polar 5–An electron accelerator experiment within an aurora, 1-4, *Planet. Space Sci., 28*, 259, 1980.

Melzner, F., G. Metzner, and D. Antrack, The GEOS electron beam experiment S 329, *Space Sci. Instrum., 4*, 45, 1978.

Neubert, T., W.W.L. Taylor, L.R.O. Storey, N. Kawashima, W.T. Roberts, D.L. Reasoner, P.M. Banks, D.A. Gurnett, R.L. Williams, and J. Burch, Waves generated during electron beam emissions from the space shuttle., *J. Geophys. Res., 91*, 11,321 1986.

Obayashi, T., N. Kawashima, K. Kuriki, N. Nagatomo, K. Ninomiya, S. Sasaki, A. Ushirokawa, I. Kudo, M. Ejiri, W.T. Roberts, R. Chappell, J. Burch, and P.M. Banks, Space experiments with particle accelerators (SEPAC), in *Artificial Particle Beams in Space Plasma Studies*, edited by B. Grandal, p659, Plenum, New York, 1982.

Raitt, W.J., P.M. Banks, W.F., Denig, and H.R. Anderson, Transient effects in beam-plasma interactions in a space simulation chamber stimulated by a Fast Pulse Electron Generator., in *Artificial Particle Beams in Space Plasma Studies*, edited by B. Grandal, p405, Plenum, New York, 1982.

Sasaki, S., N. Kawashima, K. Kuriki, M. Yanagisawa, and T. Obayashi, Vehicle charging observed in SEPAC spacelab-1 experiment., *J. Spacecr. Rockets*, 23, 194, 1986.

Shawhan, S.D., Description of the Plasma Diagnostics Package (PDP) for the OSS–1 shuttle mission and JSC chamber test in conjunction with the Fast Pulse Electron Generator (FPEG), in *Artificial Particle Beams in Space Plasma Studies*, edited by B. Grandal, p419, Plenum, New York, 1982.

Shawhan, S.D., G.B Murphy, and J.S. Picket, Plasma Diagnostics Package initial assessment of the STS 3 orbiter plasma environment, *J. Spacer. Rockets, 21*, 387, 1984a.

Shawhan, S.D., G.B. Murphy, and D.L. Fortna, Measurements of electromagnetic interference on OV102 *Columbia* using the Plasma Diagnostics Package, *J. Spacer. Rockets, 21*, 392, 1984b.

Winckler, J.R., J.E. Steffen, P.R. Malcolm, K.N. Erickson, Y. Abe, and R.L. Swanson, Ion resonances and ELF wave production by an electron beam injected into the ionosphere: Echo 6, *J. Geophys. Res., 89*, 7565, 1984.

Winckler, J.R., The application of artificial electron beams to magnetospheric research, *Rev. Geophys., 19*, 659, 1980.

Winckler, J.R., K.E. Erickson, Y. Abe, J.E. Steffen, and P.R. Malcolm, ELF Wave production by an electron beam emitting rocket system and its suppression on auroral field lines, *Geophys. Res. Lett., 12*, 457, 1985.

P.M. Banks, R.I. Bush, A.C. Fraser-Smith, T. Neubert, and G.D. Reeves, STAR Laboratory, Durand 202, Stanford University, Stanford CA 94305.

D.A. Gurnett, Department of Physics and Astronomy, University of Iowa, Iowa City, IA 52242.

W.J. Raitt, Center for Atmospheric and Space Science, Utah State University, Logan, UT 84322

(received May 4, 1987;
revised August 31, 1987;
accepted September 2, 1987.)